

Measurements of crossed-field demagnetisation rate of trapped field magnets at high frequencies and below 77 K

A Baskys¹ , A Patel¹  and B A Glowacki^{1,2} 

¹ Applied Superconductivity and Cryoscience Group, Department of Materials Science and Metallurgy, University of Cambridge, 27 Charles Babbage Road, Cambridge, CB3 0FS, United Kingdom

² Institute of Power Engineering, ul. Mory 8, 02-981 Warsaw, Poland

E-mail: ab857@cam.ac.uk

Received 19 January 2018, revised 27 March 2018

Accepted for publication 18 April 2018

Published 11 May 2018



Abstract

Design requirements of the next generation of electric aircraft place stringent requirements on the power density required from electric motors. A future prototype planned in the scope of the European project ‘Advanced Superconducting Motor Experimental Demonstrator’ (ASuMED) considers a permanent magnet synchronous motor, where the conventional ferromagnets are replaced with superconducting trapped field magnets, which promise higher flux densities and thus higher output power without adding weight. Previous work has indicated that stacks of tape show lower cross-field demagnetisation rates to bulk (RE)BCO whilst retaining similar performance for their size, however the crossed-field demagnetisation rate has not been studied in the temperature, the magnetic field and frequency range that are relevant for the operational prototype motor. This work investigates crossed-field demagnetisation in 2G high temperature superconducting stacks at temperatures below 77 K and a frequency range above 10 Hz. This information is crucial in developing designs and determining operational time before re-magnetisation could be required.

Keywords: trapped field magnets, stack of HTS tapes, crossed-field

(Some figures may appear in colour only in the online journal)

1. Introduction

Stacks of superconducting tape layers can be used as magnetic field sources in the same way as (RE)BCO bulks by circulating a persistent current within the sample. Very recently it was demonstrated that such stacks can trap fields of 17.7 T [1] matching and exceeding the performance of bulk superconductors. This is in comparison to conventional ferromagnets, which are limited to magnetic fields of about 1.5 T regardless of their size. Moreover, just like (RE)BCO bulks,

stacks of (RE)BCO tape can be used for passive magnetic levitation in high speed contactless bearings [2].

The high trapped fields demonstrate the possibility of incorporating such superconducting magnets in motors and generators. However, stacks in applications experience an AC magnetic field that causes demagnetisation [3–6], and although this effect can be used for reducing shielding currents in superconducting magnets [7] it is detrimental when stacks are used as trapped field magnets in motors or generators. Despite this, experimental studies for characterising the effect at likely operating conditions for such applications are still lacking.

Figure 1 shows a simplified picture of the external AC field experienced by a stack in applications. The field can be decomposed into perpendicular and parallel field components. The effect of the B_{aACy} component on trapped field magnets is



Original content from this work may be used under the terms of the Creative Commons Attribution 3.0 licence. Any further distribution of this work must maintain attribution to the author(s) and the title of the work, journal citation and DOI.

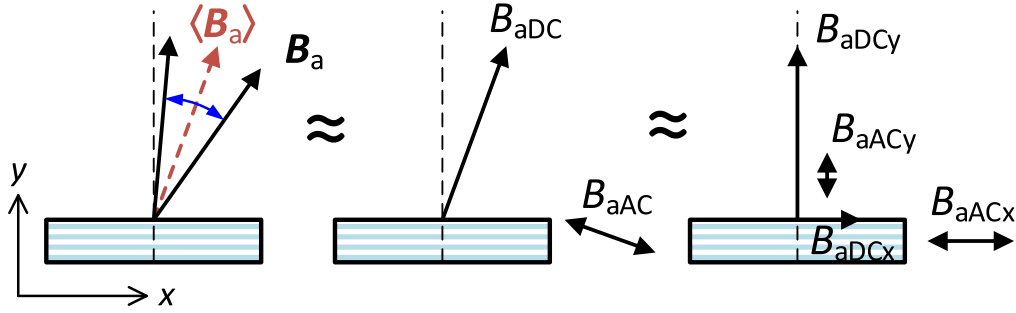


Figure 1. External field experienced by the high temperature superconducting (HTS) stack in a motor application.

relatively well studied and understood [8, 9]. When an external alternating field is applied in the y direction, to an already magnetised sample with a magnitude below the full penetration field, the flux moves in and out of the sample at the periphery, but the current distribution in the interior of the sample does not fundamentally change. If the temperature of the sample can be kept constant, no further decrease in magnetisation would be expected. If the temperature of the sample is allowed to increase (followed by decrease in critical current density), the external field penetrates further and further inside the sample resulting in decreasing magnetisation. Nevertheless, this can be mitigated by effective cooling.

On the other hand, when the direction of the external applied field is perpendicular to the tape layers B_{aACx} , in the case of stacks of HTS tape, even a small applied field exceeds the penetration field of a single tape in that orientation, which reduces the magnetisation along the y axis. However, there is data [4] suggesting that the demagnetisation rate is actually slower in stacks of tape than in bulk superconductors. The effect B_{aACx} is less well understood from a theoretical standpoint, but it is a major challenge, and cannot be solved by increased cooling to maintain stable temperature. The large aspect ratio of the individual tape layers presents complications for numerical simulations and experimental data at low temperatures and high frequencies is lacking. Therefore, in this work we focus on demagnetisation due to B_{aACx} component, which will be referred to as the applied crossed-field, B_a .

2. Methods and techniques

2.1. Superconducting tape and tape stacks

The 2G HTS tape was purchased from SuperOx with average critical current, I_c of 475 A at 77 K and self-field, for the tape layers tested. The tape is comprised of 12 mm wide, 60 μm thick Hastelloy substrate, $\sim 2 \mu\text{m}$ (RE)BCO layer and $\sim 2 \mu\text{m}$ thick Ag over-layer. The tape was cut to $12 \times 12 \text{ mm}$ square pieces for making stacks. The number of layers in the stack was varied for the measurements as described in the following sections.

2.2. Measurement system

The measurement system is schematically depicted in figure 2(a). It is comprised of a vacuum walled glass fibre reinforced epoxy (G10) cryostat cooled by helium vapour. The cryostat is partially inserted into a helium dewar and the helium vapour flow is controlled by a heater inside the dewar. The heater (and the temperature) is controlled by a proportional-integral-derivative control algorithm implemented in labVIEW. Samples were field-cooled using an iron-cored Walker Scientific HV-4H electromagnet with 2 inch diameter field poles, producing a field of up to 1.2 T. The sample is then moved to the centre of the copper solenoid below where the crossed-field is applied. The sample is allowed 5 min after magnetisation before the crossed-field is applied. Due to logarithmic time dependency of the flux creep, after the 5 min interval the relaxation rate dramatically slows down.

It was chosen to apply the crossed-field in a separate air-cored solenoid to avoid any influence of the iron, as it does affect the relaxation rate of the TFM and the lower inductance allows for driving the coil at much higher frequencies. The crossed-field coil was cooled by liquid nitrogen.

The experiment was controlled by a custom made labVIEW program. The crossed-field coil was driven by a harmonic signal from Agilent 33220A signal generator amplified by two KEPCO BOP 2020 power supplies in series set up for current control. Some capacitance was introduced in series to the coil to lower the impedance of the circuit for specific frequencies tested. The current magnitude and its waveform through the coil was measured and the using LEM Ultrastab IT 405-S current transducer.

The sample probe contains an Arepoc Hall sensor LHP-MPc for measuring the trapped field and a carbon ceramic temperature sensor for monitoring the temperature. The active area of the Hall sensor is centred above the stack 1.1 mm above its surface. The overview of the measurement system is depicted in figure 2(b).

A slightly simpler version of the cryostat was made for measurements at 77 K and was simply filled with liquid nitrogen.

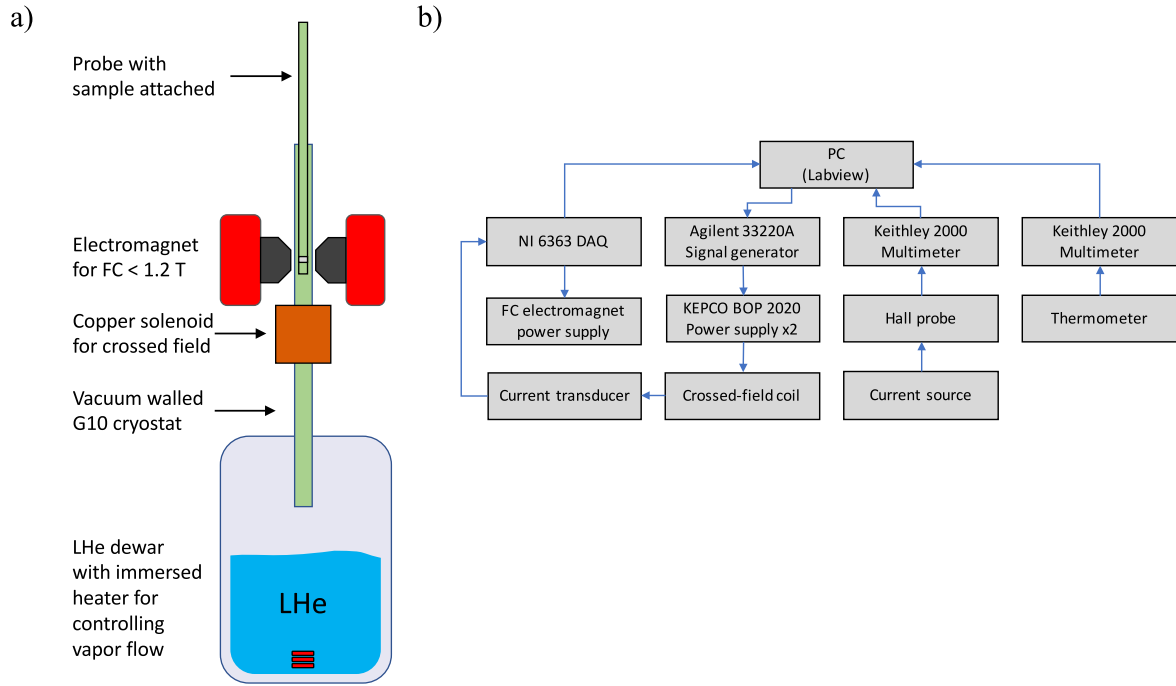


Figure 2. Overview of the measurement system used in this work (a) and the simplified diagram of the measurement and data acquisition equipment (b).

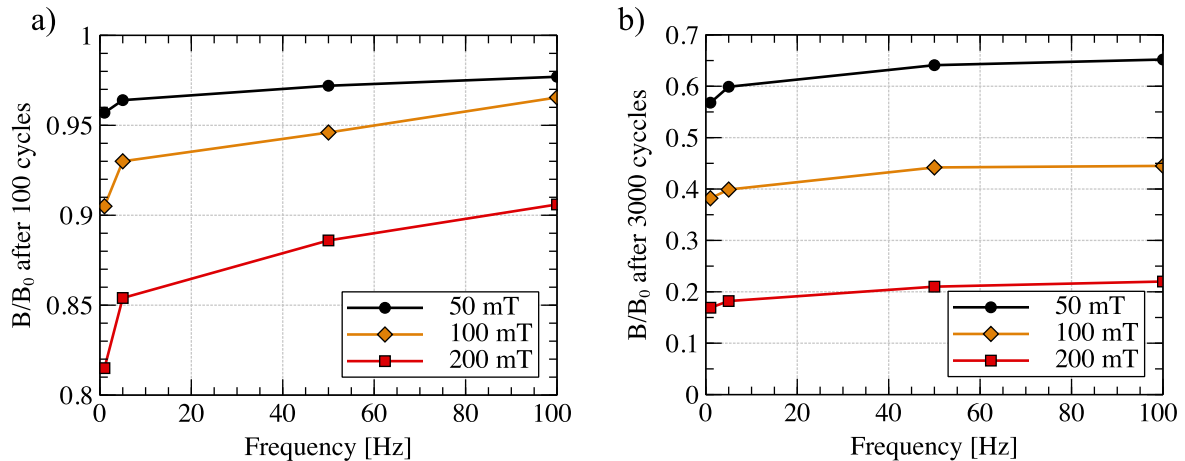


Figure 3. The normalised flux density above the TFM after (a) 100 and (b) 3000 cycles of applied crossed-field at various frequencies.

3. Experimental results

3.1. Decay rate dependency on crossed-field frequency (77 K)

Previously reported measurements have determined a trapped field decay rate (per cycle) dependence on frequency of the applied crossed-field [4] in the frequency range of 0.5–2.5 Hz, however another study by [6] showed little dependency in the low frequency range of ~15–100 mHz range and finite element simulations of the effect did not predict a frequency dependence for 40–500 Hz range. The theory by Brandt and Mikitik [10, 11] does not predict a frequency dependence either. However, no experimental verification has been done in the frequency range of $f \sim 100$ Hz, which is of interest for many rotating machines. For a synchronous motor with n field poles per phase, the number of revolutions per minute is given

by $\text{rpm} = 120f/n$ and for typical values of n , this corresponds to several thousand rpm.

The results in figure 3 show the normalised flux density above the stack after 100 and 3000 cycles for applied crossed-field amplitude in the range of 50–200 mT and frequency range from 1 to 100 Hz. The sample measured was a 20-layer stack, and measurement was done at 77 K.

It can be seen that the frequency of applied field does not affect the trapped field significantly. There seems to be a small variation in the decay rate at low frequencies (1–5 Hz), however it is most likely due to flux creep, as the low frequency tests take much longer to complete the same number of cycles. Flux creep over a period of an hour, can contribute up to 3% of decrease in measured field. The fact that frequency does not change the decay rate (per cycle), allows us

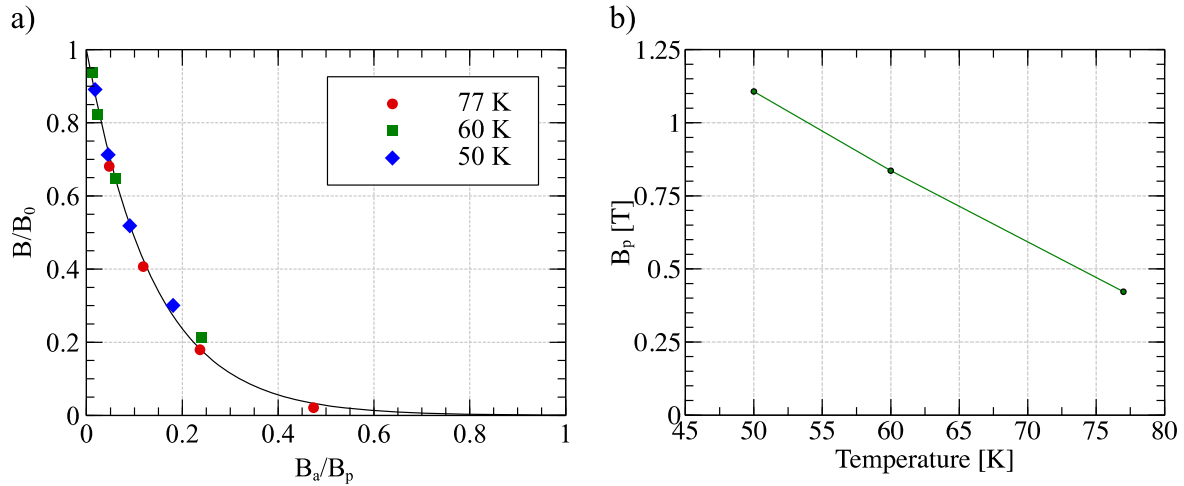


Figure 4. Normalised trapped field in a 20-layer stack after 10^4 cycles of applied crossed-field at 50 Hz (a). The applied field magnitude is normalised by the penetration field at that temperature. The penetration field determined by modelling is shown in (b).

to perform subsequent experiments at higher frequencies that allow collecting data for many applied crossed-field cycles in short period of time. Specifically, the subsequent measurements were performed at 50 Hz. However, it is worth noting that in applications, the decay rate (per unit of time) gets linearly worse with frequency.

3.2. Decay rate dependency on crossed-field magnitude and temperature

The same 20-layer stack from 3.1 was then tested at temperatures below 77 K. In order to fully saturate the sample with 1.2 T (limitation of the electromagnet) for field cooling, temperatures only down to 50 K were considered. The results for the remaining flux density after 10^4 cycles for various applied fields at 77, 60 and 50 K are plotted in figure 4(a). The trapped flux density is normalised by the trapped field before application of crossed-field, B_0 . Moreover, the applied crossed-field is normalised by the penetration field, B_p (field necessary to induce the current through the sample, or the maximum trapped field in the centre of the sample at the specified temperature). Although it is the penetration field parallel to the plane of the tape (direction x in figure 1), B_{pX} , that is of interest, it is not trivial to measure, nor to estimate due to the extreme aspect ratio of the individual tape layers. Nevertheless, the penetration field perpendicular to tape layers (or along the plane normal of the tape), B_{pY} , is expected to scale with B_{pX} . Therefore, for simplicity, it was chosen as the scaling parameter $B_{pY} \equiv B_p$. The penetration field was estimated numerically using an FEM model described elsewhere [12]. The model takes into account the critical current dependency on magnetic field magnitude and sample temperature, $J_c(B, T)$. The critical current data was taken from [13], however, relatively few data points are available across the temperature range, hence linear interpolation was used. The penetration field is plotted in figure 4(b).

Figure 4(a) shows that the results lie on the same curve irrespective of the temperature, thus the remnant field B/B_0 for the given stack depends only on the ratio of applied field

and penetration field. The penetration field in turn is determined by the critical current characteristics $J_c(B, T)$. The curve in figure 4(a) is an exponential function of form consistent with results in [10].

To test this to even lower temperatures, the stack was reduced to five layers, which allows us to fully saturate the sample with 1.2 T applied field down to 20 K. More systematic study, applying 20% of B_p at each temperature. The results for the temperature range 20–77 K and various number of applied cycles are summarised in figure 5(a). The results also show very little dependency with temperature, other than that due to $B_p(T)$ (see figure 5(b)). This again allows us to estimate the behaviour of the stack just based on measurements on 77 K and $J_c(B, T)$ data. This simplifies the picture tremendously as measurements are much easier to make at liquid nitrogen temperatures.

3.3. Number of layers

It was shown before by modelling [5] and experiment [6] that increasing the number of layers in the stack may reduce the demagnetisation rate. Results of a similar experiment are shown here as well, see figure 6. The measurements were done at 77 K in liquid nitrogen and the applied crossed-field was 20% of the B_p in each case. Again by scaling the applied field by B_p , we can see that the reduction in demagnetisation rate is due to increase in B_p as the number of layers in the stack increases.

There is some variation for low tape number count and high number of applied cycles, however this may be due to error in B_p estimation. For such low number of layers, the variation in $J_c(B, T)$ in the individual layers is more significant and for the $J_c(B, T)$ data at very low field, the effect self-field during $J_c(B, T)$ measurements may be significant [14]. Nevertheless, for practical purposes, the layer count in the stack is going to be much higher than 10, to achieve appreciable trapped fields.

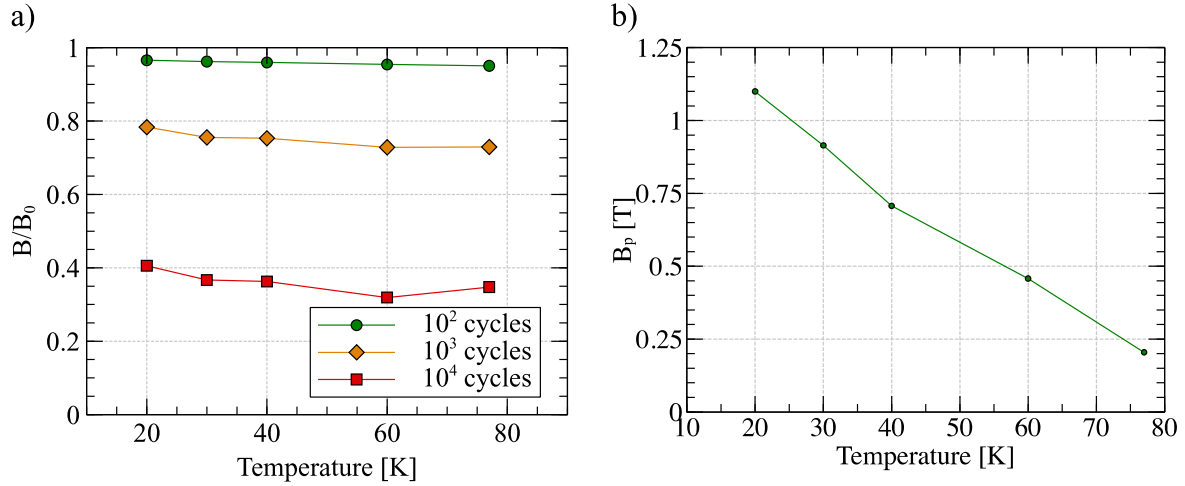


Figure 5. Normalised trapped field in a five-layer stack after applying crossed-field with amplitude equal to 20% of B_p for 10^2 , 10^3 and 10^4 cycles (a). The penetration field $B_p(T)$ determined by modelling shown in (b).

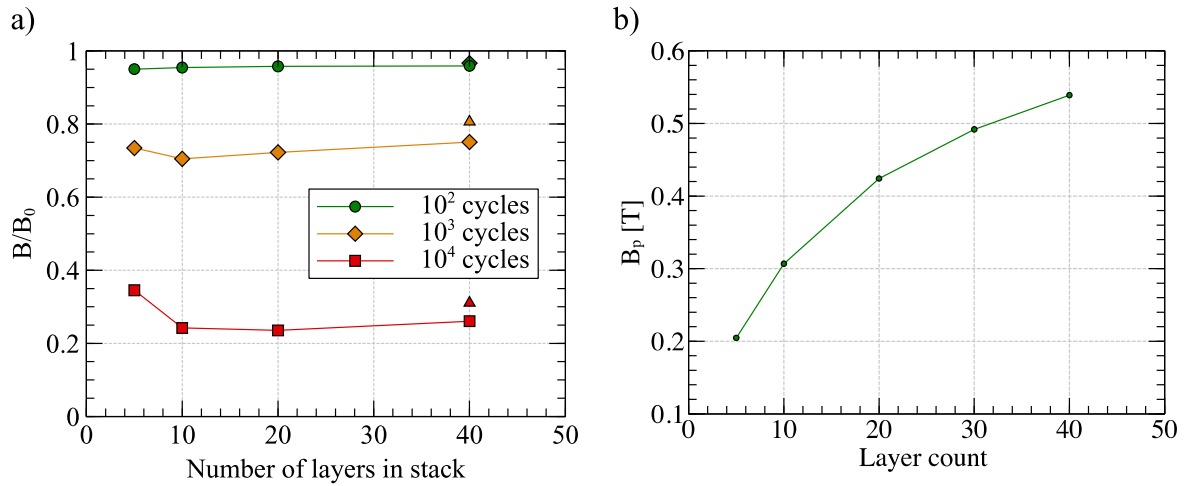


Figure 6. The normalised trapped field at 77 K above stacks with varying number of tape layers after 10^2 , 10^3 and 10^4 cycles of applied crossed-field (a). The triangle-shaped data points are tests where the samples were field-cooled with applied field only 50% of B_p . In each case, the magnitude of the crossed-field was 20% of penetration field B_p . Variation of B_p with the number of layers in the stack (modelling) is shown in (b).

Moreover, the data points in triangle markers show that non-saturated stacks (field-cooled in a field that is only 50% of B_p , show slightly lower demagnetisation rate).

3.4. Reduction of demagnetisation rate

The most obvious way to reduce the demagnetisation rate for a given stack operating at a particular temperature, is to shield the applied crossed-field. Several approaches for this were suggested by Baghdadi *et al* [15] that involve wrapping the stack of tapes with perpendicular layers of superconducting tape and Mu metal that has high magnetic permeability.

A similar strategy was experimentally tried as a proof-of-concept. A 20-layer stack was used and four layers of the same HTS tape, were cut to 4 mm thin strips and placed perpendicularly to the stack the applied crossed-field as shown in figure 7(a). The side layers were not centred to the stack to make the top surface clear as it would be in an application. The side layers are expected to shield at least a

portion of the stack from the external applied field as illustrated in figure 7(b). The figure shows the magnetic field distribution in the volume of the tape stack when a flux density of 20 mT is applied. The shielding capacity, just as the flux trapping capacity of stacks of tape, depends on the number of layers in the stack and the width of the tape layers in relation to the volume of space that need to be shielded.

The experimental results for normalised trapped field decay in crossed-field with and without side layers for shielding are plotted in figure 8. The solid lines represent the trapped field without the shielding and dashed lines with the shielding added. It is apparent that the side layers do have a positive effect for small applied fields <100 mT. This is unsurprising, as only four layers of tape were used for shielding.

Nevertheless, the shielding did provide some reduction in the demagnetisation rate and a more detailed study, using different geometries for the shielding tape as well as layers of ferromagnetic materials is under way. Moreover, the side

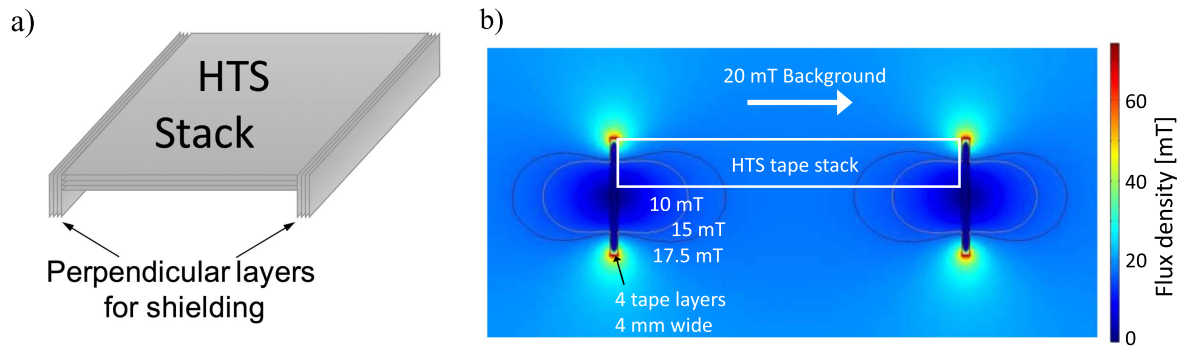


Figure 7. Sample arrangement including the stack of tapes along with the side tapes for shielding the crossed-field (a) and the simulation of flux density distribution in the volume of the HTS tape stack when a 20 mT external field is applied (b), showing that at least some of the volume is partially shielded by the side tapes.

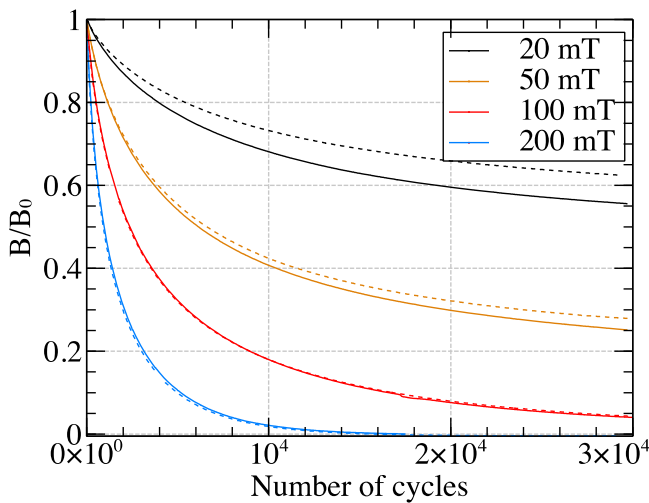


Figure 8. Normalised flux density above the 20-layer stack after application of crossed-field with magnitudes from 20 to 200 mT. Solid lines are for samples without and dashed lines—with the shielding side tapes, as in figure 7(a).

layers did not affect the measured field above the stack after magnetisation, which remained 179 ± 2 mT at 77 K.

The effect of the induced eddy currents in the Hastelloy substrate and silver stabiliser were considered, but simulations show that the effect is negligible at 50 Hz, as the silver stabiliser is only $2 \mu\text{m}$ thick, whilst the Hastelloy has conductivity that is two orders of magnitude lower than silver.

4. Conclusions

The demagnetisation may prove to be a critical issue when designing applications where stacks of tape, or more generally - trapped field magnets, are used. The decay rate does slow down over time, however, it has not been shown to asymptote to a constant value. Nevertheless, the work presented here shows that B_a/B_p is the parameter of importance, and it is important to keep this parameter as low as possible when designing applications. Moreover, applications operating at high frequencies are more susceptible to faster demagnetisation of trapped field magnets.

It is worth noting that the real operating environment in e.g. a real motor, is significantly different from the experimental setup detailed in this work. Most notably, it is likely that there will be ferromagnetic materials in the near vicinity of the TFMs which will affect the field distribution and hence the demagnetisation rate. The applied field configuration is also far more complicated with the field pole experiencing field gradients along the surface and AC magnetic field components in both parallel and perpendicular orientations with respect to the TFM. Moreover, field poles are expected to be much wider than 12 mm to enable higher trapped flux densities. This means that the tapes will likely be curved to conform to the rotor. The effect of curvature and larger width still needs to be investigated in future work. Nevertheless, given that so far, modelling has produced only qualitative results, it may be needed to test the TFMs in conditions as close to the actual application as possible, or even *in situ* in a prototype. One such prototype is currently being constructed in the ASCG laboratory, University of Cambridge.

Acknowledgments

This work was funded by an EPSRC grant EP/P000738/1.

ORCID iDs

A Baskys <https://orcid.org/0000-0002-1875-8106>

A Patel <https://orcid.org/0000-0002-3979-3517>

B A Glowacki <https://orcid.org/0000-0003-2165-6378>

References

- [1] Patel A, Baskys A, Mitchell-Williams T, McCaul A, Coniglio W and Glowacki B A 2017 A trapped field of 17.7 T in a stack of high temperature superconducting tape arXiv:1709.04541
- [2] Patel A, Kalitka V, Hopkins S C, Baskys A, Albisetti A F, Giunchi G, Molodyk A and Glowacki B A 2016 Magnetic levitation between a slab of soldered HTS tape and a

- cylindrical permanent magnet *IEEE Trans. Appl. Supercond.* **26** 3601305
- [3] Vanderbemden P, Hong Z, Coombs T A, Denis S, Ausloos M, Schwartz J, Rutel I B, Hari Babu N, Cardwell D A and Campbell A M 2007 Behavior of bulk high-temperature superconductors of finite thickness subjected to crossed magnetic fields: experiment and model *Phys. Rev. B* **75** 174515
 - [4] Baghdadi M, Ruiz H S and Coombs T A 2014 Crossed-magnetic-field experiments on stacked second generation superconducting tapes: reduction of the demagnetization effects *Appl. Phys. Lett.* **104** 232602
 - [5] Campbell A, Baghdadi M, Patel A, Zhou D, Huang K Y, Shi Y and Coombs T 2017 Demagnetisation by crossed fields in superconductors *Supercond. Sci. Technol.* **30** 034005
 - [6] Liang F, Qu T, Zhang Z, Sheng J, Yuan W, Iwasa Y and Zhang M 2017 Vortex shaking study of REBCO tape with consideration of anisotropic characteristics *Supercond. Sci. Technol.* **30** 094006
 - [7] Lee J, Park D, Michael P C, Noguchi S, Bascunan J and Iwasa Y 2018 A field-shaking system to reduce the screening-current-induced field in the 800 MHz HTS insert of the MIT 1.3 GHz LTS/HTS NMR magnet: a small-model study *IEEE Trans. Appl. Supercond.* **28** 4301405
 - [8] Zushi Y, Asaba I, Ogawa J, Yamagishi K, Tsukamoto O, Murakami M and Tomita M 2004 Study on suppression of decay of trapped magnetic field in HTS bulk subject to AC magnetic field *Physica C* **412–414** 708–13
 - [9] Ogawa J, Iwamoto M, Yamagishi K, Tsukamoto O, Murakami M and Tomita M 2003 Influence of AC external magnetic field perturbation on trapped magnetic field in HTS bulk *Physica C* **386** 26–30
 - [10] Brandt E H and Mikitik G P 2002 Why an ac magnetic field shifts the irreversibility line in type-II superconductors *Phys. Rev. Lett.* **89** 27002
 - [11] Mikitik G P and Brandt E H 2003 Theory of the longitudinal vortex-shaking effect in superconducting strips *Phys. Rev. B* **67** 104511
 - [12] Baskys A, Patel A, Hopkins S and Glowacki B 2016 Modeling of trapped fields by stacked (RE)BCO tape using angular transversal field dependency *IEEE Trans. Appl. Supercond.* **26** 6601004
 - [13] Wimbush A 2017 A high-temperature superconducting (HTS) wire critical current database (<https://doi.org/10.6084/m9.figshare.c.2861821.v6>)
 - [14] Zermeno V M R, Habelok K, Stępień M and Grilli F 2017 A parameter-free method to extract the superconductor's $J_c(B, \theta)$ field-dependence from in-field current–voltage characteristics of high temperature superconductor tapes *Supercond. Sci. Technol.* **30** 034001
 - [15] Baghdadi M, Ruiz H S, Fagnard J F, Zhang M, Wang W and Coombs T A 2015 Investigation of demagnetization in HTS stacked tapes implemented in electric machines as a result of crossed magnetic field *IEEE Trans. Appl. Supercond.* **25** 6602404